Structural Perfection in Physisorbed Films: A Synchrotron X-Ray Diffraction Study of Xenon Adsorbed on the Ag(111) Surface

P. Dai,[1] T. Angot,[1,*] S. N. Ehrlich,[2,†] S.-K. Wang,[1] and H. Taub[1]

[1]*Department of Physics and Astronomy, University of Missouri-Columbia, Columbia, Missouri 65211*

[2]*School of Materials Engineering, Purdue University, West Lafayette, Indiana 47907*

(Received 2 August 1993)

Synchrotron x-ray scattering has been used to investigate the structure and growth of xenon films physisorbed on the Ag(111) surface. For growth under quasiequilibrium conditions, the bulk Xe-Xe spacing is reached at monolayer completion and fcc films of thickness ≥ 220 Å are observed. Under kinetic growth conditions, intensity oscillations in the specular reflectivity as a function of time demonstrate nearly layer-by-layer growth. Modeling of the intensity at a fixed coverage allows profiling of the Xe/vacuum interface as well as a direct determination of the film's thickness and layer spacings.

PACS numbers: 68.35.Bs, 61.10.−i, 68.55.Gi, 68.55.Jk

Synchrotron x-ray diffraction has developed rapidly in recent years as a technique for *in situ* monitoring of surface structure during film growth. The method has been applied to layer-by-layer growth at semiconductor [1,2] and metal surfaces [3] as well as at a metal-semiconductor interface [4]. These experiments have exploited the extreme brilliance of synchrotron x-ray sources as well as high resolution in reciprocal space to follow the structural evolution of the surface region from monolayer thickness to bulk [5].

Rare gases physisorbed on single-crystal metal surfaces offer some of the most appealing films to model theoretically [6–8] due to the simplicity of the adatom-adatom and adatom-substrate interactions. These films provide a benchmark for the degree of understanding which one can hope to achieve for other physisorbed films. Unfortunately, synchrotron x-ray diffraction studies of the structure and growth of physisorbed films have lagged behind those on semiconductor and metal surfaces. Most of the previous experiments on rare gas films have been performed on graphite substrates, for which capillary condensation effects [6,9] or a high degree of stacking disorder [10] have obscured the multilayer structure of the film. Thus, despite the remarkable simplicity of these prototypical films, a number of basic questions remain unresolved: (1) Are successive layers of the film identical in structure? (2) What is the spacing between layers; are they mutually commensurate, and, if so, what is their stacking sequence? And (3) what is the ultimate film thickness and what are the principal defects determining it?

Here we report some recent synchrotron x-ray scattering studies of xenon films adsorbed on the Ag(111) surface under both quasiequilibrium and kinetic growth conditions. Our use of single-crystal substrate without a polycrystalline ballast for coverage determination eliminates capillary condensation effects [11] and allows films to be grown with a higher degree of structural perfection than previously achieved [10]. In probing the multilayer structure of the Xe film inaccessible to low-energy electron diffraction (LEED) [7] and He atom scattering [12] techniques, significant progress has been made in addressing the unresolved questions enumerated above. Specifically, we are able to make the most precise comparison to date of the lattice constant in successive film layers with that of bulk Xe, determine the layer spacings and stacking sequence in the film, directly measure the ultimate film thickness, and characterize the Xe/vacuum interface by estimates of layer occupancies.

We chose the Xe/Ag(111) system for a number of reasons. Xenon has the largest x-ray cross section of the rare gases and had already been used in synchrotron diffraction studies of monolayer melting on the Ag(111) surface [13]. The comprehensive LEED studies of rare gas adsorption by Webb and co-workers [7] had established the structure and thermodynamic properties of the Xe monolayer and, to a lesser extent, the bilayer. Since the corrugation of the adatom-substrate potential is substantially less for Xe/Ag(111) than on graphite and there is a large mismatch between the lattice constants of the Xe monolayer and the Ag(111) surface [7], registry effects seen for the first Xe layer during multilayer growth on graphite [10] should be minimized.

Our experiments were performed at beam line X18A at the National Synchrotron Light Source using a double (flat) Si(111) monochromator to select an incident x-ray wavelength of 1.2208 Å and a Ge analyzer in the scattered beam, yielding a longitudinal, transverse, and out-of-plane resolution width (FWHM) of 1.0×10^{-3}, 1.7×10^{-4}, and 8.3×10^{-2} Å^{-1}, respectively. Our ultrahigh vacuum chamber and preparation of the Ag sample (10 mm diameter, miscut $<0.2°$, $\sim$900 Å coherence length) have been described previously [11]. Below 80 K, the sample temperature was measured by a Au-chromel thermocouple with an absolute uncertainty of ±2 K, while temperature differences could be measured to ±0.2 K.

Following the approach developed in earlier LEED studies [7], we began our x-ray experiments by growing films under quasiequilibrium conditions [11]. With the chamber mounted on the x-ray diffractometer, films were prepared by exposing the Ag(111) surface to a constant flux of Xe gas (99.9995% minimum purity) from a dosing

0031-9007/94/72(5)/685(4)$06.00

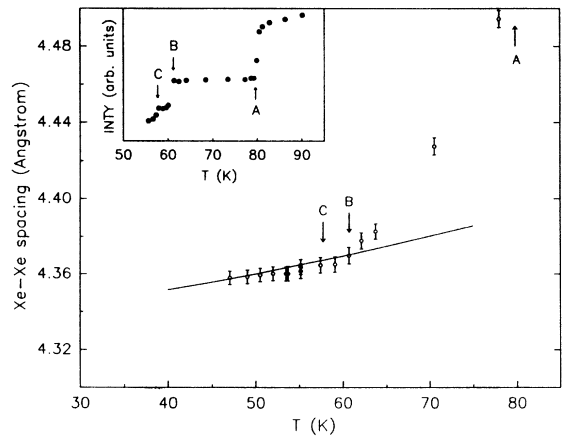

FIG. 1. The Xe-Xe spacing as a function of temperature for a Xe film in equilibrium with a constant Xe flux. Inset shows the Ag(10) LEED spot intensity observed under the same conditions. In both plots, arrows mark condensation of the first layer (A), the second layer (B), and bulk (C).

tube situated 1 cm in front of the substrate. Typically, a background Xe pressure of $\sim 1.7\times10^{-7}$ Torr would be maintained in the chamber as the substrate was cooled slowly from a temperature of $\sim$85 K and the intensity of the Ag(10) LEED spot recorded. As shown in the inset to Fig. 1 [7,11], sharp drops in the LEED intensity can be resolved at monolayer, bilayer, and bulk condensation (labeled A, B, and C, respectively). In this way, precise determination of monolayer and bilayer Xe coverage could be made without resorting to a gas ballast [10].

At monolayer coverage, radial and transverse x-ray scans through the Xe(10) diffraction rod [11] confirm the results of previous LEED [7] and x-ray [13] experiments of a hexagonal lattice incommensurate but aligned with the substrate. The Xe(10) rod had an in-plane azimuthal width (full width at half maximum) of (3-6)° which was much larger than the 0.17° measured for the Ag(10) rod in agreement with previous experiments [13]. Figure 1 shows the Xe-Xe spacing in the film versus temperature for one of several runs compared with that measured by x-ray diffraction for bulk Xe (solid line) [14]. Consistent with earlier LEED results [7,15], we find that by bilayer onset the Xe-Xe spacing in the film has reached that of the bulk to within our accuracy of ± 0.004 Å.

In none of the radial scans used to determine the Xe-Xe spacing in Fig. 1 did we observe a splitting of the Xe(10) rod indicative of a different lattice constant in successive layers of the film as suggested by some computer simulations [16]. The radial peaks at all film thicknesses could be well fitted by a Lorentzian-squared line shape as found previously [11,13]. Attributing the radial width of the Xe(10) rod to a finite coherence length L in the film (the instrumental contribution to the width is negligible), we infer $L\sim300$ Å at bilayer onset which increases by $\sim$30% at both lower and higher coverages. From modeling of the radial line shape of the Xe(10) rod at bilayer onset, we estimate the difference between the lattice constants of the monolayer and bilayer at coexistence to be ≤ 0.005 Å, comparable to calculations [8].

Common to previous surface x-ray experiments on semiconductors and metals [1-4] has been the demonstration of layerwise growth by the observation of intensity oscillations in the reflected x-ray beam as a function of time. The amplitude of these oscillations is a sensitive measure of structural perfection in the surface region. To search for these oscillations, we grew films kinetically, i.e., by subjecting the substrate held at a fixed temperature (≤ 46 K) to a constant flux of Xe gas. The x-ray diffractometer was modified for these experiments to allow specular reflection of the x-ray beam from the sample within our UHV chamber [17]. Also, the x-ray wavelength was decreased to 1.00 Å and the analyzer crystal was removed from the scattered beam. In this geometry, the longitudinal, transverse, and out-of-plane resolution widths (FWHM) became 5.6×10^{-2}, 3.9×10^{-3}, and 3.8×10^{-2} Å^{-1}, respectively.

The time dependence of the intensity at the Xe "anti-Bragg" point of the specular rod [indexed $(00\frac{3}{2})$ with respect to a hexagonal Xe unit cell] is shown in Fig. 2 for different temperatures of the Ag substrate. Intensity oscillations whose amplitude weakens with time are observed at all three temperatures. Although routinely observed in semiconductor and metal film growth, such oscillations have not been observed previously with physisorbed films, nor do other techniques, such as ellipsometry [6], allow one to predict how many oscillations might be observed. At 43 and 46 K, about four periods can be discerned which correspond to the adsorption of eight Xe layers, as will be explained below. The growth rate is $\sim$10 min/layer with the oscillation period constant to $\leq$10%. Only one complete oscillation is observed at the lowest attainable temperature of 33 K. Presumably, this is due to a slower diffusion rate at this temperature which results in a growth front spanning more than one layer.

To achieve a more quantitative understanding of these oscillations, film growth at 43 K was terminated at points labeled A, B, C, and D in Fig. 2(b) corresponding to approximate Xe film thicknesses of 1, 2, 3, and 10 layers. After cooling the sample to 33 K, specular reflectivity scans were then performed at these coverages as shown in Fig. 3. The reflectivity scans for the first three layers in Figs. 3(a) to 3(c) show the N-fold modulation expected for an N-layer film. This behavior was not observed for Xe multilayers physisorbed on single-crystal graphite [10] which apparently were structurally less perfect. It should also be noted that the specular reflectivity measurements on a graphite substrate are hampered by the Xe(00l) scattering sitting on the wing of the graphite (002) peak [10].

We have analyzed the specular reflectivity scans kinematically with a simple one-dimensional model to

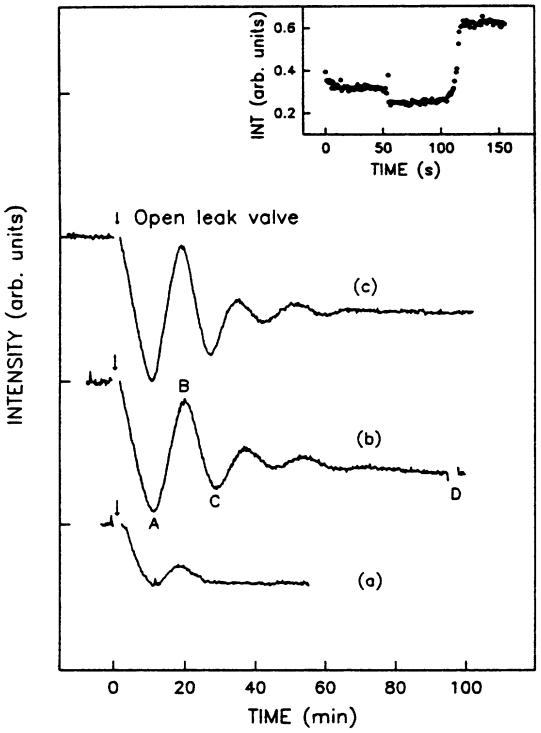

FIG. 2. Time dependence of the x-ray intensity at the Xe(00$\frac{3}{2}$) point for various substrate temperatures: (a) 33 K, (b) 43 K, and (c) 46 K. After opening the leak valve, a constant Xe dosing rate is maintained, corresponding to a background pressure in the chamber of $\sim 5.9\times10^{-8}$ Torr. In (b), points labeled *A*, *B*, *C*, and *D* correspond to an approximate Xe film thickness of 1, 2, 3, and 10 layers, respectively. Inset shows the x-ray intensity during desorption of a 1.2-layer Xe film as discussed in the text.

determine the film thickness and layer occupancies. The Xe film is assumed to consist of N complete layers above which are partial layers θ_i ($\theta_i \leq 1$, $i=1,2,3$); d_{AgXe} denotes the spacing between the first Xe layer and the Ag substrate, and d_{Xe} and d_{Ag} the spacings between adjacent film and substrate layers, respectively. In general, there will be both sharp (Bragg) and diffuse contributions to the diffracted intensity near the specular rod [1,18]. Describing the substrate reflectivity by a crystal truncation rod [19] and ignoring constant prefactors, we can express the Bragg intensity for a film with a single partial layer as [1]

$$I=\left|\frac{f_{\mathrm{Xe}}}{a_{\mathrm{Xe}}^2}\left[\frac{1-e^{iNq_\perp d_{\mathrm{Xe}}}}{1-e^{iq_\perp d_{\mathrm{Xe}}}}e^{iq_\perp d_{\mathrm{AgXe}}}+\theta_1 e^{iq_\perp(d_{\mathrm{AgXe}}+Nd_{\mathrm{Xe}})}\right]+\frac{f_{\mathrm{Ag}}}{a_{\mathrm{Ag}}^2(1-e^{iq_\perp d_{\mathrm{Ag}}})}\right|^2\delta(q_\parallel)\,, \quad (1)$$

where $f_{\mathrm{Ag}}, a_{\mathrm{Ag}}$ and $f_{\mathrm{Xe}}, a_{\mathrm{Xe}}$ are the atomic form factor and lattice constant for Ag and Xe, respectively, and $q_\perp$ and $q_\parallel$ are the wave vector transfer perpendicular and parallel to the surface, respectively. The first term in Eq. (1) is contributed by the film, while the second term represents the Ag(10) crystal truncation rod.

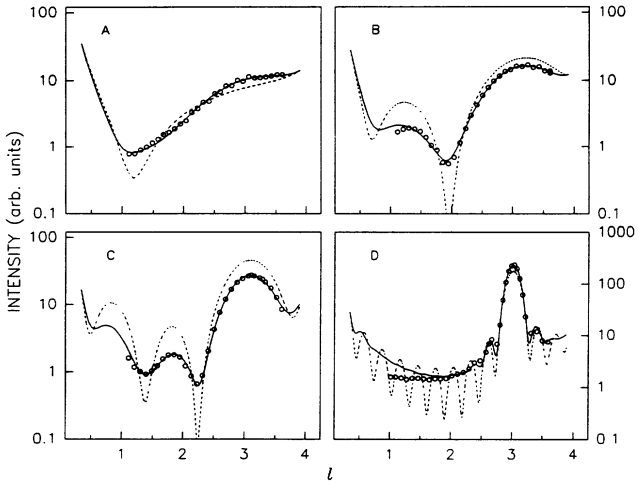

FIG. 3. Specular reflectivity (00*l*) scans (open circles) at 33 K for Xe film thicknesses corresponding to points labeled *A*, *B*, *C*, and *D* in Fig. 2(b). At each point, the intensity has been integrated transverse to the rod. Note logarithmic intensity scale and, on the horizontal axis, l is in units of 0.59 Å^{-1}. Calculated reflectivity after corrections for illuminated sample area and Lorentz-polarization factor: dashed lines correspond to film thicknesses of exactly 1, 2, 3, and 10 layers for (a), (b), (c), and (d), respectively; solid curves are best fits obtained assuming up to 3 partial layers as discussed in the text.

The specular scan at nominal one-layer coverage plotted on a log scale cannot be well fitted by Eq. (1) with $\theta_1=0$ as shown by the dashed curve in Fig. 3(a). However, the fit improves with a value of $\theta_1=0.2$ as shown by the solid curve. Strong support for this model is provided by the desorption experiment shown in the inset to Fig. 2. The intensity at the Xe anti-Bragg point is plotted vs time as the sample is heated at this coverage. The first drop in reflectivity corresponds to desorption of the partial second layer while the subsequent intensity rise occurs at monolayer desorption after which the reflectivity of the bare substrate is recovered. The value of $\theta_1=0.2$ is quantitatively consistent with the percentage drop observed at desorption of the partial second layer. It is interesting to note that desorption experiments of this type cannot be performed with more strongly bonded semiconductor and metal films [1–4].

If the film growth is strictly layer by layer, it can be seen from Eq. (1) that the intensity at the Xe(00$\frac{3}{2}$) point of the specular rod will have a parabolic dependence on coverage rather than the decaying sinusoidal oscillation shown in Fig. 2. This suggests that more than 1 partial layer is present during the growth process. Extending Eq. (1) to the case of 2 partial layers on top of N complete Xe layers, we find that the specular scan at a coverage of nominally 2 layers in Fig. 3(b) can be well fitted with parameters $N=1$, $\theta_1=0.64$, and $\theta_2=0.08$ (solid curve). This fit is substantially better than that as-

suming exactly 2 layers (dashed curve). Similarly, assuming 3 partial layers, we improve the fit to the specular scan at nominally three-layer coverage and obtain parameters $N=1$, $\theta_1=0.80$, $\theta_2=0.62$, and $\theta_3=0.12$. Fixing $d_{Xe}=3.54$ Å and $d_{Ag}=2.35$ Å (their bulk values), the fits to the specular scans in Figs. 3(b) and 3(c) yield the same value of $d_{AgXe}=3.55\pm0.1$ Å as obtained from a dynamical analysis of LEED experiments [20,21].

At a coverage of ~10 layers, the absence of intensity oscillations at the Xe$(00\frac{3}{2})$ point in Fig. 2(d) and the presence of only two secondary maxima in the specular scan of Fig. 3(d) suggest that the number of partial layers continues to increase as the film thickens. Rather than introduce more parameters θ_i in Eq. (1), we have used a simpler model to analyze the specular reflectivity. It considers independently scattering columns consisting of an integer number of Xe layers and the underlying Ag substrate. The column heights are assumed to have a Gaussian distribution with a mean column height $\bar{h}$ and standard deviation σ_h. As shown by the solid curve in Fig. 3(d), this model significantly improves the fit over that for 10 complete layers (dashed curve) and yields the values of $\bar{h}=10.5$ and $\sigma_h=2$. The value of $d_{AgXe}=3.54$ Å obtained from the fit agrees well with that of 3.55 Å inferred at lower coverages.

To summarize this analysis of the specular reflectivity, our values of the average film thickness above 2 layers are relatively insensitive to the models employed, depending primarily on the positions of the intensity extremae, and hence provide a significant improvement over previous estimates based on deposition time or thermal desorption [7,12]. Although values of the layer occupancies may be more model dependent, it is clear from both this analysis and the attenuation of oscillations at the anti-Bragg point that there is an increasing number of partial layers in the films as they thicken. Thus our results demonstrate that the growth front of thin Xe films spans more than 1 layer and allow a characterization of the Xe/vacuum interface which has eluded previous experiments [7,9,10]. Further studies of the roughening of rare gas films during growth as well as the multilayer structure of other physisorbed films are in progress.

Although space does not permit a discussion here [22], we have performed diffraction scans along the Xe$(01l)$ rod at coverages above 2 layers and observed peaks consistent with the "*ABC*" stacking sequence of an fcc structure. For films grown under quasiequilibrium conditions, the peak widths correspond to film thicknesses exceeding 220 Å or ~63 layers.

We wish to thank P. F. Miceli, I. K. Robinson, L. W. Bruch, M. B. Webb, J. Z. Larese, J. M. Phillips, F. Y. Hansen, and B. M. Ocko for helpful discussions. This work was partially supported by U.S. National Science Foundation Grants No. DMR-8704938 and No. DMR-9011069 (H.T.) and U.S. Department of Energy Grant No. DE-FG02-85ER45183 of the MATRIX Participating Research Team (S.N.E. and H.T.).

*Present address: Groupe de Physique des États Condensés, URA CNRS 783, Case 901, Faculté des Sciences de Luminy, 13288 Marseille Cedex 9, France.

†Present address: NSLS, Brookhaven National Laboratory, Upton, NY 11973.

[1] E. Vlieg, A. W. Denier van der Gon, J. F. van der Veen, J. E. Macdonald, and C. Norris, Phys. Rev. Lett. **61**, 2241 (1988).

[2] P. H. Fuoss, D. W. Kisker, F. J. Lamelas, and G. B. Stephenson, Phys. Rev. Lett. **69**, 2791 (1992).

[3] H. A. van der Vegt, H. M. van Pinxteren, M. Lohmeier, E. Vlieg, and J. M. C. Thornton, Phys. Rev. Lett. **68**, 2539 (1992).

[4] P. A. Bennett, B. DeVries, I. K. Robinson, and P. J. Eng, Phys. Rev. Lett. **69**, 3335 (1992).

[5] R. Feidenhans'l, Surf. Sci. Rep. **10**, 105 (1989).

[6] See, for example, G. B. Hess, in *Phase Transitions in Surface Films 2*, edited by H. Taub, G. Torzo, H. J. Lauter, and S. C. Fain, Jr., NATO Advanced Study Institute, Ser. B, Vol. 267 (Plenum, New York, 1991), p. 357.

[7] J. Unguris, L. W. Bruch, E. R. Moog, and M. B. Webb, Surf. Sci. **87**, 415 (1979), and references cited therein.

[8] L. W. Bruch and X.-Z. Ni, Faraday Discuss. Chem. Soc. **80**, 217 (1985); M. S. Wei and L. W. Bruch, J. Chem. Phys. **75**, 4130 (1981).

[9] J. Z. Larese, Q. M. Zhang, L. Passell, J. M. Hastings, J. R. Dennison, and H. Taub, Phys. Rev. B **40**, 4271 (1989).

[10] H. Hong and R. J. Birgeneau, Z. Phys. B **77**, 413 (1989).

[11] J. R. Dennison, S.-K. Wang, P. Dau, T. Angot, H. Taub, and S. N. Ehrlich, Rev. Sci. Instrum. **63**, 3835 (1992).

[12] K. D. Gibson and S. J. Sibener, J. Chem. Phys. **88**, 7862 (1988); J. Chem. Phys. **88**, 7893 (1988); K. D. Gibson, C. Cerjan, J. C. Light, and S. J. Sibener, J. Chem. Phys. **88**, 1911 (1988).

[13] N. Greiser, G. A. Held, R. Frahm, R. L. Greener, P. M. Horn, and R. M. Suter, Phys. Rev. Lett. **59**, 1706 (1987).

[14] *Rare Gas Solids*, edited by M. L. Klein and J. A. Venables (Academic, New York, 1977), Vol. II.

[15] Note that the Xe-Xe spacing of the thick film has not been normalized to the bulk value of Ref. [14] as was done in Ref. [7]. The relative precision of our Xe-Xe spacing measurements is ±0.001 Å.

[16] J. M. Phillips, Langmuir **5**, 571 (1989).

[17] S.-K. Wang, P. Dai, and H. Taub, J. Appl. Cryst. **26**, 697 (1993).

[18] Because of the out-of-plane mosaic of the Ag(111) substrate, the Bragg component is spread over an angular range of $\sim0.3°$. The diffuse contribution is neglected in this simple model.

[19] I. K. Robinson, Phys. Rev. B **33**, 3830 (1986).

[20] N. Stoner, M. A. Van Hove, S. Y. Tong, and M. B. Webb, Phys. Rev. Lett. **40**, 243 (1978).

[21] Since data were not taken at small enough l values to locate the intensity minimum in the near monolayer scan [Fig. 3(a)], the value of $d_{AgXe}=3.64$ Å inferred from it is believed to be less reliable.

[22] P. Dai, Z. Wu, T. Angot, S. N. Ehrlich, S.-K. Wang, and H. Taub (unpublished).